

UNIVERSITY OF BUCHAREST
FACULTY OF CHEMISTRY
DOCTORAL SCHOOL IN CHEMISTRY

PhD THESIS ABSTRACT

**AFFINITY-BASED BIOSENSORS FOR DOPING
APPLICATIONS**

PhD student:

George - Mădălin DĂNILĂ

PhD Supervisor:

Prof. Dr. Camelia BALA

Doctoral committee:

President: Prof. dr. Andrei-Valentin Medvedovici

Supervisor: Prof. dr. Camelia BALA

Jury:

1. Prof. dr. Ion Ion, *POLITEHNICA* University, Bucharest
2. CS I habil. dr. Gheorghiu Eugen, International Centre of Biodynamics, Bucharest
3. Conf. habil. dr. Gligor Delia Maria, Babeş-Bolyai University, Cluj-Napoca

2022

Table of contents

1	Theoretical part	12
1.1	The main class of substances used for performance enhancement	12
1.2	Ghrelin - the “hunger” hormone. Interaction with growth hormone secretagogue receptor.....	13
1.2.1	Ghrelin mimetics	17
1.2.2	Receptor agonists, antagonists and inverse agonists. Mechanism of action	18
1.3	Cannabinoids.....	22
1.3.1	Metabolic pathways.....	23
1.3.2	Specific interaction with cannabinoid receptors. Allosteric modulation	25
1.4	Detection methods for receptor’s extracellular ligands.....	27
1.4.1	Agonists.....	27
1.4.2	Antagonists and inverse agonists	28
1.4.3	Allosteric modulators - Cannabinoids.....	29
ORIGINAL CONTRIBUTIONS		
2	DETECTION OF GHSR-1a ANTAGONISTS BASED ON AFFINITY PROFILES	32
2.1	Reagents and equipment.....	34
2.2	Optimization of parameters	35
2.3	Results and discussion.....	40
2.3.1	Calibration curve of GHSR-1a receptor	40
2.3.2	Binding curve of human ghrelin to GHSR-1a receptor.....	41
2.3.3	Affinity profiles of antagonists	43
2.3.4	Affinity analysis and binding model	44
2.4	Conclusions	50
3	DETECTION OF GHSR-1a AGONISTS AND INVERSE AGONISTS BASED ON AFFINITY PROFILES	51
3.1	Reagents and equipment.....	52
3.2	Receptor immobilization and analyte detection	54
3.3	Results and discussion.....	55
3.3.1	Agonists affinity profiles.....	56
3.3.2	Inverse agonists affinity profiles	59
3.4	Conclusions	62
4	DETECTION OF NATURAL CANNABINOIDS AS ALLOSTERIC MODUALTORS OF GHSR-1a RECEPTOR BASED ON AFFINITY PROFILES	63

4.1	Reagents and equipment.....	64
4.2	Analyte detection.....	66
4.3	Results and discussion.....	67
4.3.1	Cannabinoids as allosteric modulators	67
4.3.2	Affinity profiles of allosteric modulators	68
4.3.3	Validation of affinity profiles based analytical method using direct comparison of results with gas chromatography tandem mass spectrometry	74
4.4	Conclusions	80
5	Peptide molecular-wire biosensor for electrochemical detection of doping agents.....	82
5.1	Reagents and equipment.....	83
5.2	Biosensor development	84
5.3	Circular dichroism and Atomic Force Microscopy studies.....	88
5.4	Affinity assays.....	89
5.5	Results and discussion.....	89
5.5.1	Design of the peptide bridge	89
5.5.2	Optimization of the pre-treatment procedure	91
5.5.3	Characterization of the peptide bridge	92
5.5.4	Estimation of electron transfer kinetic parameters.....	94
5.5.5	Stability of the peptide layer	102
5.5.6	Characterization of sensor's surface	103
5.5.7	Detection of GHSR-1a receptor	106
5.5.8	Reproducibility, anti-interference, and selectivity studies	108
5.6	Conclusions	111
6	GENERAL CONCLUSIONS AND FUTURE PERSPECTIVES.....	112
7	PUBLISHED PAPERS	115
8	REFERENCES.....	117

INTRODUCTION

The major goal of the PhD thesis was the development of immunoanalytical and electrochemical alternatives to chromatographic detection of ghrelin mimetics. In this context, the doctoral research was focused on the development of assay formats that would allow the early detection of the analytes, as *screening* methods with rapid response indicating the presence / absence of the doping substance, like point-of-care (POC) applications. Since no specific antibodies for these novel mimetics have been reported so far, the challenge was also to investigate the affinity profile of analytes in direct competition with labelled ghrelin for the binding sites of the growth hormone secretagogue receptor (GHS-R1a), the only biomolecule available for ligand recognition.

The doctoral thesis is divided into two parts: a theoretical (chapter 1) and an original part (comprising chapters numbered from 2 to 5).

The theoretical section contains four subchapters, with emphasis on the class of substances and growth factors that include ghrelin, the endogenous ligand of GHS-R1a, and ghrelin mimetics.

The original contributions section, divided into four chapters, presents the experimental results obtained during the PhD stage, being organized according to the compounds' subclasses. Therefore, **Chapter 2** is focused on the detection of the secretagogue receptor antagonists (generic names D-Lys³-GHRP-6, YIL-781, and L-692,585), exploiting their affinity profiles in competitive assays in the presence of the GHSR-1a receptor.

In the following chapter (**Chapter 3**), an agonist (CJC-1295-DAC) and an inverse agonist (D-Arg¹, D-Phe⁵, D-Trp^{7,9}, Leu¹¹]-Substance P) were studied in competitive assays with peroxidase-labelled ghrelin.

Chapter 4 contains the experimental reporting the allosteric effect of natural cannabinoids such as cannabidiol and the major metabolite of tetrahydrocannabinol, carboxy-THC on the GHS-R1a activity, for the first time in the scientific literature. The interaction of cannabinoids with the GHSR-1a receptor was studied using the ghrelin mimetics detection format (presented in **Chapters 2** and **Chapter 3**), as well as the kinetic model for estimating the affinity constants.

The final chapter, **Chapter 5**, describes the development of a modular peptide-based biosensor for the detection the GHSR-1a receptor, exploiting the specific binding to the immobilized peptide agonist CJC-1295-DAC. The biosensor is characterized by several voltametric techniques (cyclic voltammetry, square wave, alternating current, and electrochemical impedance spectroscopy), surface investigation techniques (atomic force microscopy), and circular dichroism analysis of peptide layer deposited on the electrode surface. The modular design

of the peptide biosensor, as well as the electrochemical characterization of CJC-1295-DAC binding to its transmembrane receptor, were reported for the first time in scientific literature.

ORIGINAL CONTRIBUTIONS

Chapter 2 - Detection of GHSR-1a receptor antagonists

This chapter describes the development of a competitive assay format together with the affinity profiles of the GHSR-1a receptor antagonists, obtained in competitive assays with peroxidase-labeled ghrelin. Three antagonists have been chosen to study the affinity profiles of antagonists following their specific binding to the growth hormone secretagogue receptor: 1 peptidyl antagonist ([D-Lys³]-GHRP-6) and 2 nonpeptidyl antagonists (YIL-781 and L-692,585) (Figure 2-1).

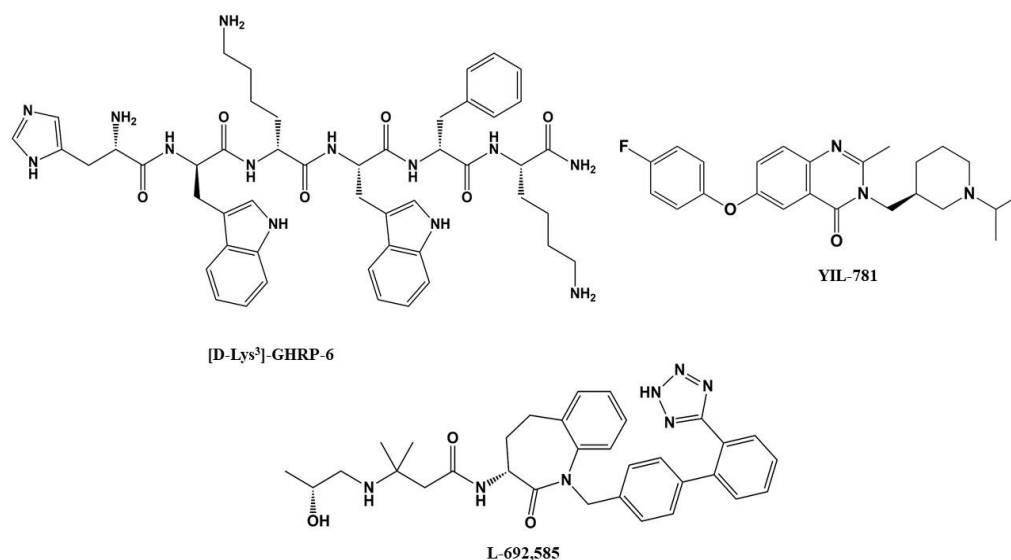


Figure Error! No text of specified style in document. -1 Chemical structure of the GHS-R1a antagonists selected for this study

Parameter optimization

Optimization of coating process

The maximal coverage of streptavidin was favored by a slightly acid buffer. For the competition experiments a 2.5 µg/mL streptavidin solution was prepared in 0.05 M citric acid / sodium acetate buffer, pH 5.0.

Optimization of blocking steps

3 blocking steps of 10 minutes, each one at room temperature, with 2.5 $\mu\text{g/mL}$ of free biotin and free streptavidin, respectively, were used to minimize non-specific binding and false positive results. The optimization results are presented in Figure 2-3.

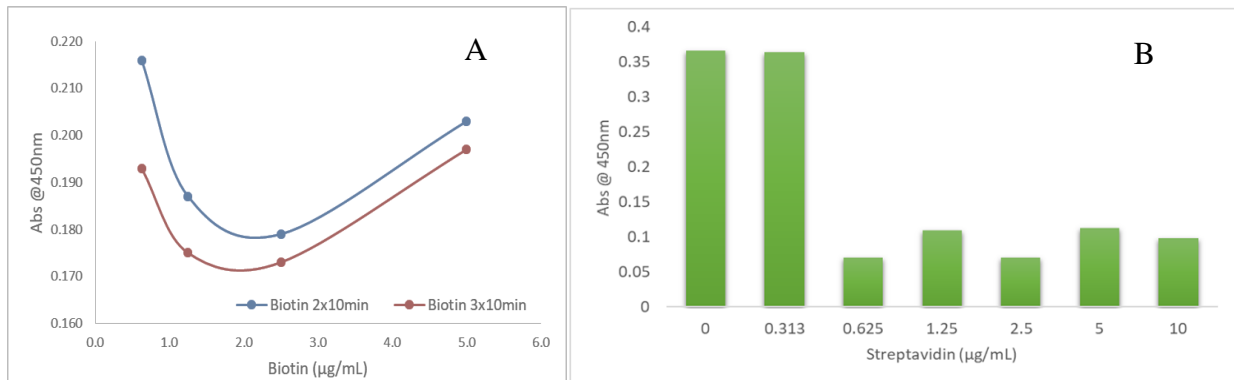


Figure Error! No text of specified style in document.-2 (A) Blocking of free binding sites of streptavidin after immobilization of antibody. Two protocols were tested: blocking with biotin with different concentrations for a) 2 times for 10 minutes and b) 3 times for 10 minutes at room temperature; (B) Blocking of biotinylated antibody anti-GHSR1a (0.5 $\mu\text{g/mL}$) after binding on surface coated streptavidin with different concentrations of free streptavidin. Blocking process was carried out in 2 steps of 10 minutes at room temperature.

Ghrelin receptor calibration curve

A calibration curve was constructed on the linear range 0.3 - 20 ng/mL using an ELISA kit developed for the detection of the GHSR-1a receptor. A concentration of 10 ng/mL of recombinant receptor resulted in an absorbance of 0,1 ng/mL on this curve, indicating that the receptor is only 1% in its active form.

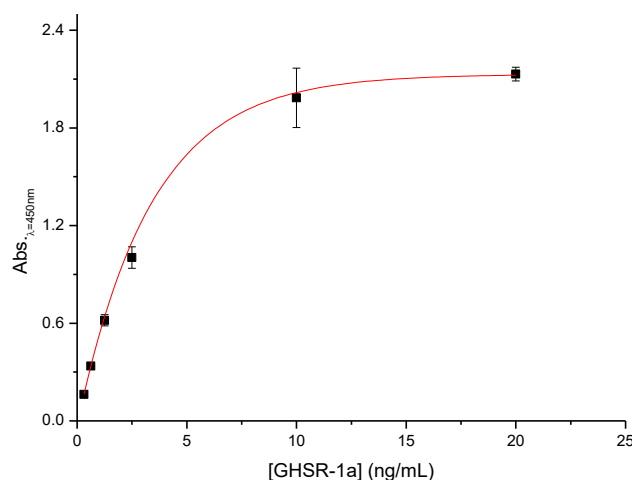


Figure Error! No text of specified style in document.-3 Calibration curve for the detection of active GHSR-1a receptor using an ELISA sandwich assay. All binding experiments were performed in 10 mM PBS buffer, pH 7.4, and 37°C

Ghrelin binding curve

Direct binding experiments with biotinylated ghrelin (bio-GHR) in the 50–1000 nM range, at various surface densities of GHS-R1a, highlighted a hyperbolic pattern of the saturation curves, characteristic to the one-site model (Figure 2-6).

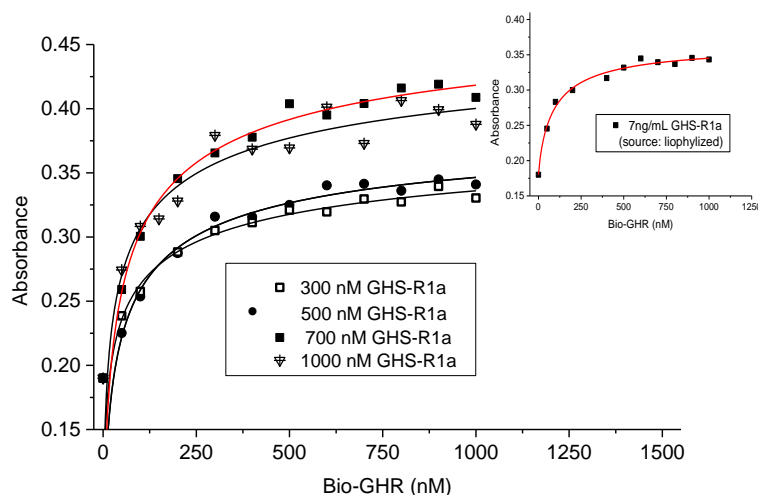


Figure Error! No text of specified style in document. **-4** Direct saturation experiments with immobilized recombinant GHS-R1a (source: wheat germ) using various concentrations of bio-GHR. The highest absorbances were achieved for 700 and 1000 nM GHS-R1a added in the immobilization step. All binding experiments were performed in 10 mM PBS buffer, pH = 7.4 and 37°C.

The experimental curves were processed through nonlinear regression analysis (Conn et al., 2009), Hill equation and biphasic model onto binding data (Puiu et al., 2018). Only the Hill equation matched the experimental data.

$$Y = a + \frac{b}{1 + \left(\frac{c}{X}\right)^d} \quad (2.2)$$

where **Y** is the absorbance measured at 450 nm (as a result of binding of bio-GHR to its receptor), **X** is the molar concentration of bio-GHR, **a** is the basal response, **b** is the maximal absorbance, **c** is half maximal effective concentration (EC_{50} , molar concentration), and **d** is the Hill coefficient (showing the number of bio-GHR molecules binding the receptor), in this case EC_{50} represents also the dissociation constant bio-GHR/GHS-R1a at 37 °C.

EC values ranged within 138–143 nM. The estimated Hill coefficients were distributed between 0.9 and 1.3, thereby confirming the one-site binding model (ghrelin is binding only at the orthosteric site).

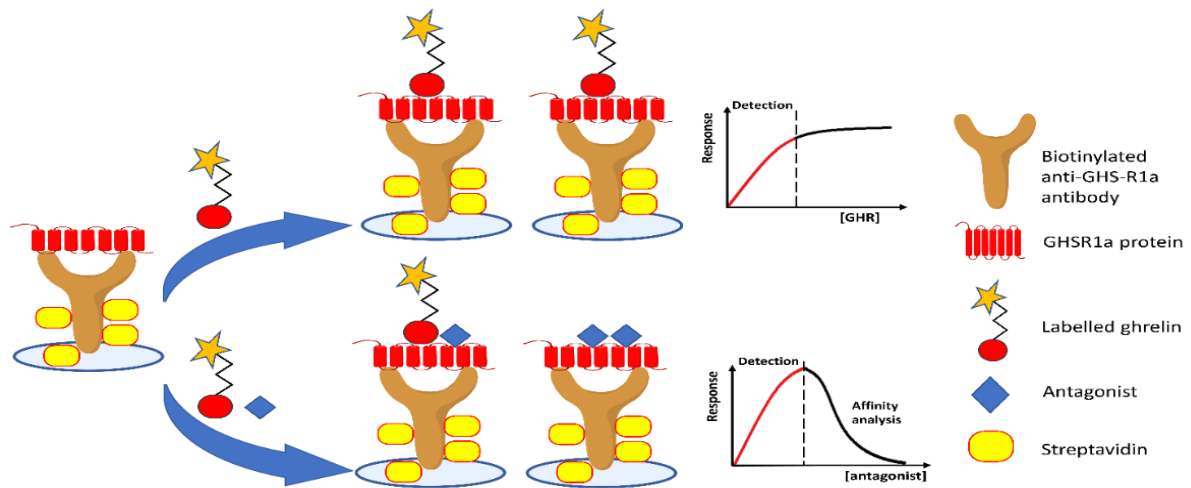


Figure Error! No text of specified style in document.-5 Schematic representation of the modular biosensing format

Affinity profiles of antagonists

The competitive assays with antagonists indicate that antagonists bind both allosteric and orthosteric site, the allosteric site being unavailable for ghrelin (Figure 2-8).

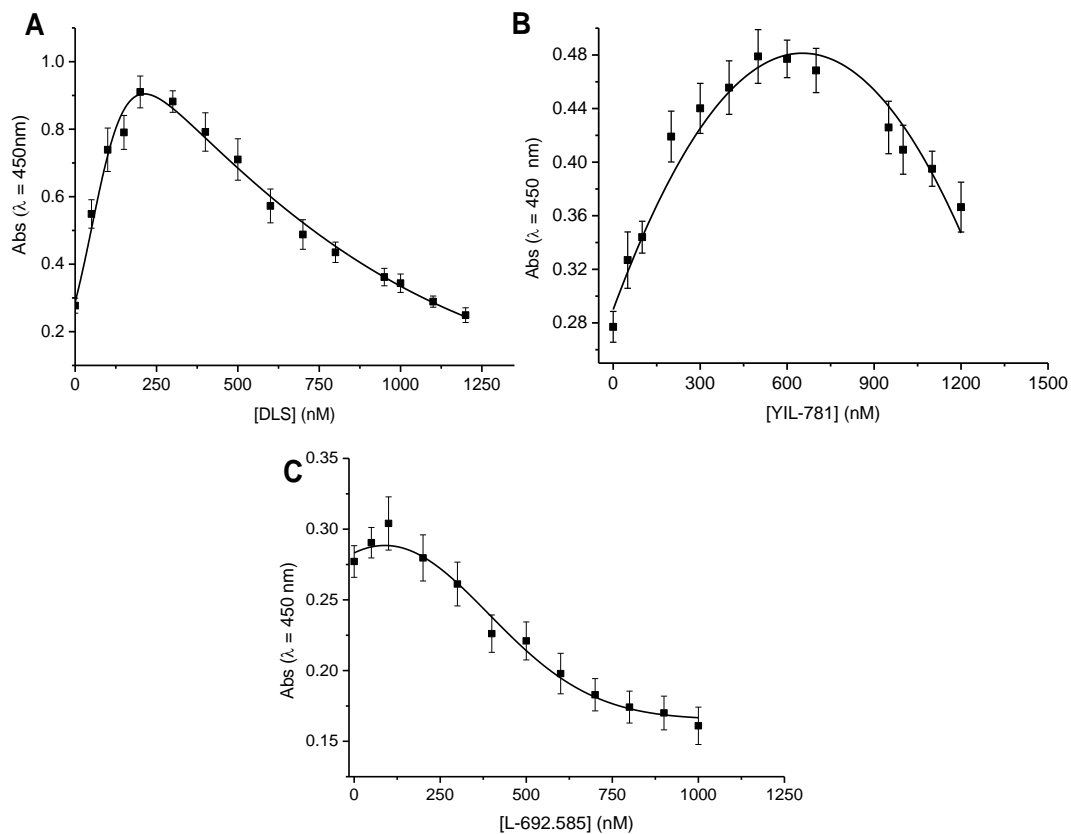


Figure Error! No text of specified style in document.-6 Competitive binding experiments involving 223 nM bio-GHR and various concentrations of (A) DLS, (B) YIL-781, and (C) L-692-585. The binding curves display bell-shaped features characteristic to allosteric modulation. All experiments were performed in 10 mM PBS buffer (pH 7.4) at 37°C.

Affinity analysis and binding model

The binding of antagonists to this specific domain in GHS-R1a favors the subsequent binding of ghrelin through allosteric modulation at low concentrations of antagonists. A sequence of equilibria (described by eqs. (2.3) - (2.8),) able to sustain the bell-shaped pattern of the binding curves in competitive assays, was used to estimate the dissociation constants:



where:

R is the GHSR-1a receptor, **G** is ghrelin, **A** represents the studied antagonist, **K₁ – K₆** are the affinity constants (association). **RA** designates the complex receptor/antagonist with **A** bound to the orthosteric site, while **RA*** is the complex resulting from the binding of **A** to the allosteric site of receptor.

Non-linear regression analysis was applied for the estimation of constants:

$$Y = \frac{a+bX}{c+dX+eX^2} \quad (2.12)$$

$$a = 3K_5(K_1 + K_2K_5)[G] \quad (2.13)$$

$$b = 2K_3K_4K_5[G] \quad (2.14)$$

$$c = 6K_5 + 3K_5(K_1 + K_2K_5)[G] \quad (2.15)$$

$$d = 3(K_2K_5 - K_1)K_5 + 2K_5K_3 + 2K_3K_4K_5[G] \quad (2.16)$$

$$e = 2K_3K_5K_6 \quad (2.17)$$

Where:

Y is the normalized absorbance, whereas **G** represents the concentration of bio-GHR in all competitive experiments (223 nM). The results obtained are presented in Table 2-2.

Table Error! No text of specified style in document.-1 Affinity/dissociation constants estimated through non-linear regression analysis using the “two-binding site” model for competitive binding assays with bio-GHR and antagonists (10 mM PBS buffer, pH 7.4 at 37°C)

Antagonist	Dissociation constant (nM)						r ²
	K ₁ ⁻¹	K ₂ ⁻¹	K ₃ ⁻¹	K ₄ ⁻¹	K ₅ ⁻¹	K ₆ ⁻¹	
DLS	89.0±6.8	1509±103	171.4±1.6	82.9±7.2	1.05±0.13	99.40±8,04	0.9851
YIL-781	89.0±6.8	2164±112	189.0±16.0	72.6±6.7	1.16±0.18	302.0±16.0	0.9872

Two binding sites can be observed for the GHSR-1a receptor, both with different affinity constants (K_2^{-1} for orthosteric site and K_3^{-1} for allosteric site). The affinity for the allosteric site of GHS-R1a seems to exceed about 1 order of magnitude the affinity for the orthosteric site in the case of DLS and YIL-781. The limit of detection (LOD) for both antagonists are 29.0 and 27.0 ng/mL, respectively. The binding curve of L-692,585 displays only a linear domain with negative slope which can be assigned to a stronger affinity of this antagonist for the orthosteric site ($K_2^{-1} = 0.63$ nM).

The LOD for DLS in the mixture of synthetic urine: PBS 1:4 (v/v) was found to be 74 ng/mL, in a linear range of 50–110 ng/mL (Figure 2-9).

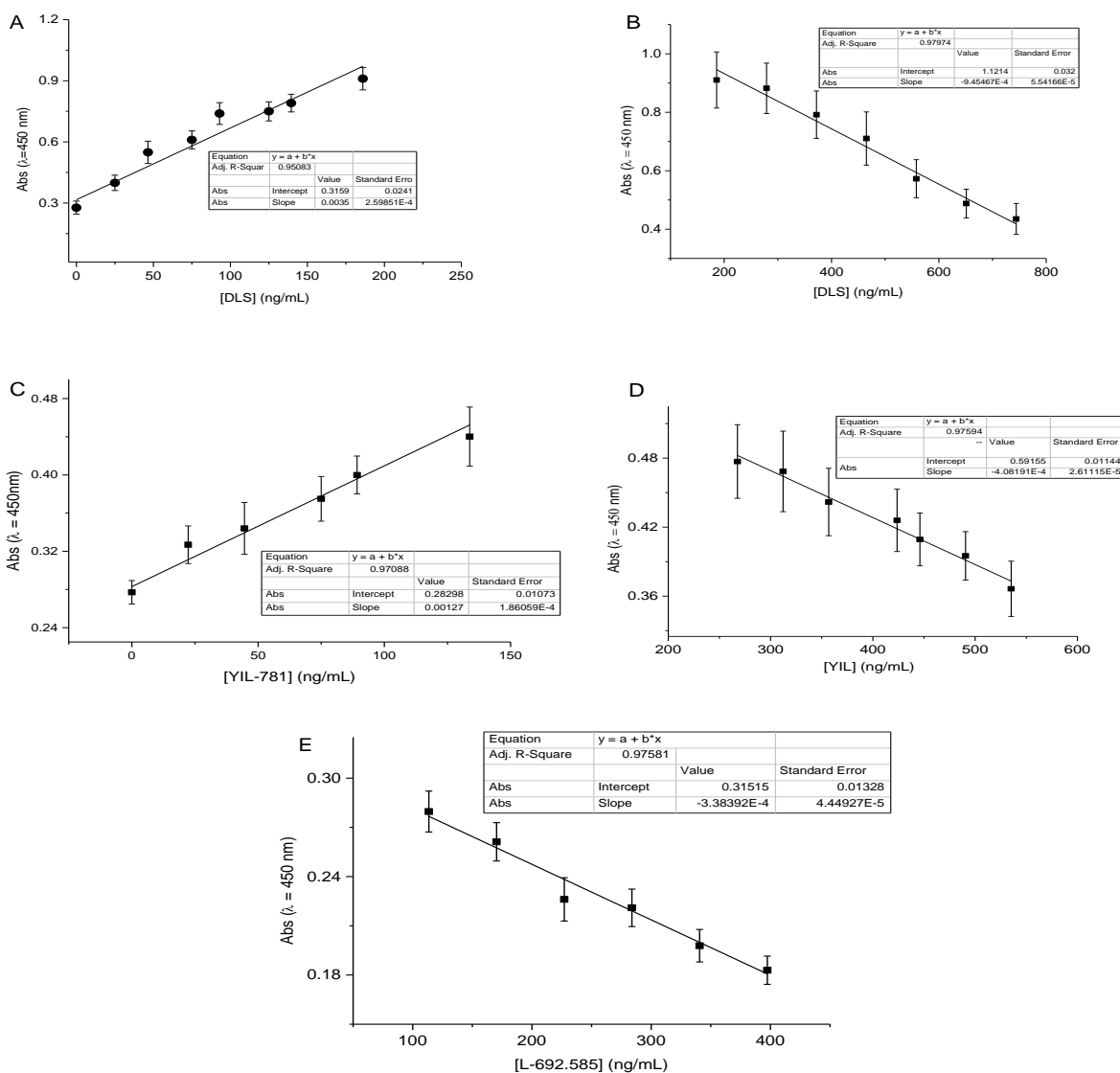


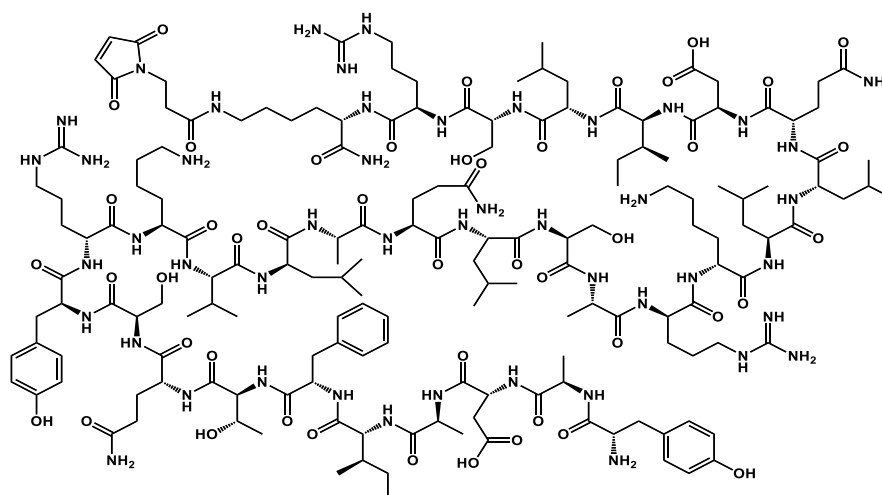
Figure 2-9 Calibration plots exploiting the linear parts of the binding curves in competitive assays with bio-GHR and antagonists. DLS exhibit a linear range with positive slope within 10-200 ng/mL (A) and a linear range with a negative slope within 200-750 ng/mL (B). A similar behavior was displayed by YIL-781 within 25-150 ng/mL (C) and 250-550 ng/mL (D). L-

692,585 can be detected using only the linear range with the negative slope (100 – 400 ng/mL) (E). All experiments were performed in 10 mM PBS buffer (pH 7.4) at 37 °C.

Chapter 3 - Detection of GHSR-1a receptor agonists and inverse agonists

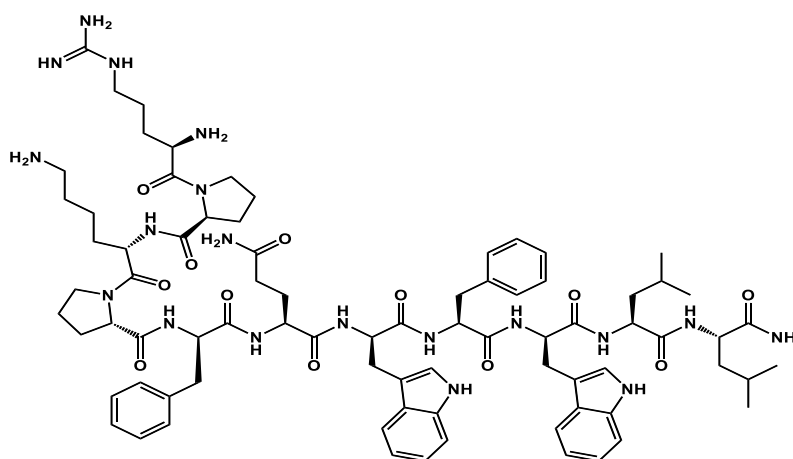
The assay format described in **Chapter 2** was applied for the detection of GHSR-1a receptor agonists. For the study of affinity profiles were selected: a peptidyl agonist CJC-1295 modified with the DAC affinity complex and an inverse agonist, [D-Arg¹,D-Phe⁵,D-Trp^{7,9}, Leu¹¹]-Substance P (Figure 3-1).

(A)



H-Tyr-D-Ala-Asp-Ala-Ile-Phe-Thr-Gln-Ser-Tyr-Arg-Lys-Val-Leu-Ala-Gln-Leu-Ser-Ala-Arg-Lys-Leu-Leu-Gln-Asp-Ile -Leu-Ser-Arg-Lys (Maleimidopropionyl)-NH₂
CJC-1295 with DAC

(B)



HD-Arg-Pro-Lys-Pro-D-Phe-Gln-D-Trp-Phe-D-Trp-Leu-Leu-NH₂
[D-Arg¹,D-Phe⁵,D-Trp^{7,9}, Leu¹¹] -Substance P

Figure Error! No text of specified style in document.-8 Chemical structures of CJC-1295-DAC agonist (A) and inverse agonist Substance P (B)

The modulating effect of agonists and inverse agonists

The modulating effect of synthetic ghrelin mimetics, CJC-1295-DAC and Substance P was studied using the affinity profiles. CJC-1295-DAC promotes the activation of GHSR-1a receptor

and subsequently the release of growth hormone from the pituitary gland. On the other hand, the agonist inhibits or reduces the constitutive activity observed at the secretagogue receptor, which is manifested even in the absence of any ligand at the orthosteric site (Holst et al., 2003).

The principle of detection based on the direct competitive format is presented in Figure 3-2.

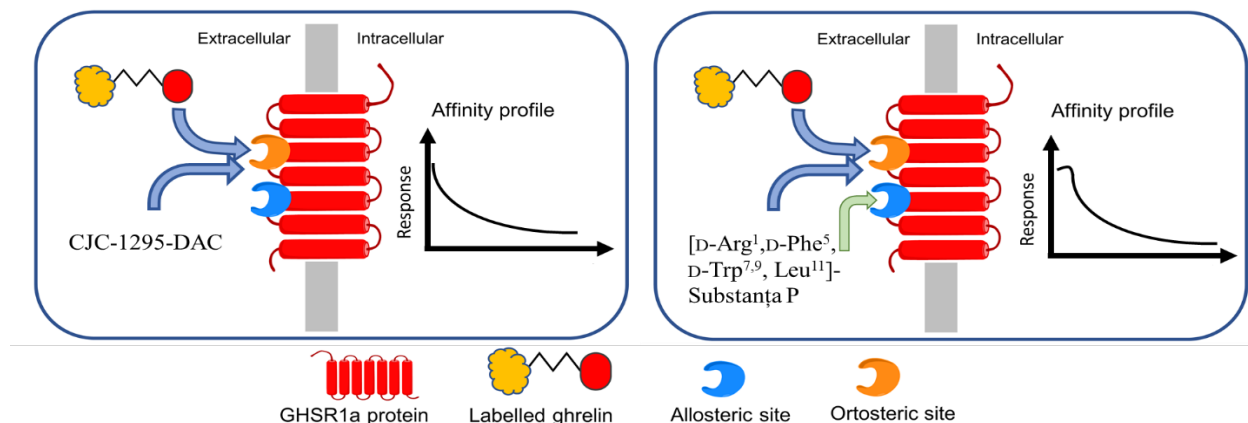


Figure Error! No text of specified style in document.-9 Schematic representation of sensing format for CJC-1295-DAC and Substance P. Although the binding curves of the system are apparently similar, the nonlinear regression analysis can discriminate between different models.

Affinity profiles of ghrelin agonists

The binding curves were analyzed using nonlinear regression and Hill equation (Sartore et al., 2020) (Figure 3-3). The peptide agonist binds at the orthosteric site of the receptor, thus competing with ghrelin.

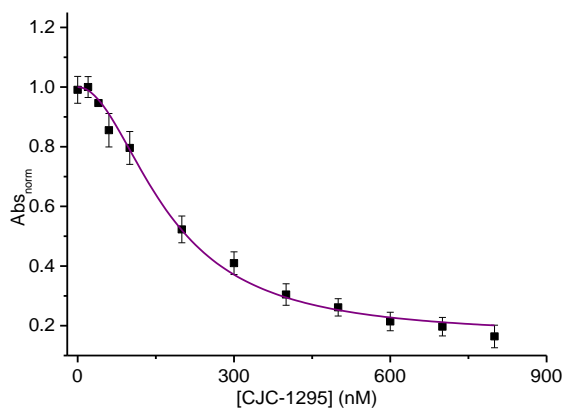


Figure Error! No text of specified style in document.-10 Affinity profiles in experiments with 223 nM bio-GHR and different concentrations of CJC-1295. All experiments were performed in triplicate in 10 mM PBS buffer, pH 7.4, at 37 °C.

The results obtained for estimating the dissociation constants are presented in Table 3-1.

Table Error! No text of specified style in document.-2 Dissociation constants estimated for CJC-1295-DAC in the corresponding systems of linear equations

Dissociation constant (nM)	CJC-1295-DAC
----------------------------	--------------

K_1^{-1} (determined in direct binding experiments with GHR)	88.90 ± 0.63
K_2^{-1} (determined in direct competitive experiments with CJC-1295-DAC)	65.80 ± 4.30

CJC-1295-DAC has a lower dissociation constant (K_2^{-1}), than the dissociation constant of ghrelin, which results in a higher affinity for the orthosteric site of the secretagogue receptor. A detection limit of 56.0 ng/mL was obtained for the CJC-1295-DAC peptide agonist in the 1:4 (v/v) mixture of synthetic urine and PBS buffer.

Affinity profiles of inverse agonists

Substance P binds both the orthosteric and allosteric site of the ghrelin receptor (Figure 3-2), with a low affinity for the orthosteric site (K_2^{-1} is much lower than K_1^{-1} for ghrelin), but also for the allosteric binding site. The estimated dissociation constant K_4^{-1} of the RA*G ternary complex (0.21 nM) confirms that the affinity with which bio-GHR binds the substance-P-activated receptor is far stronger than the affinity of the GHR/receptor complex.

Table Error! No text of specified style in document.-3 Dissociation constants for GHR and Substance P obtained either in direct or direct competitive experiments

Dissociation constant (nM)	Substance P
K_1^{-1} (determined in direct binding experiments with GHR)	88.90 ± 0.63
K_2^{-1} (determined in competitive experiments with Substance P)	$(1.23 \pm 0.11) \times 10^5$
K_3^{-1} (determined in competitive experiments with Substance P)	$(6.05 \pm 0.59) \times 10^4$
K_4^{-1} (determined in competitive experiments with Substance P)	0.210 ± 0.011
K_5^{-1} (determined in competitive experiments with Substance P)	0.538 ± 0.047
K_6^{-1} (determined in competitive experiments with Substance P)	1.230 ± 0.012

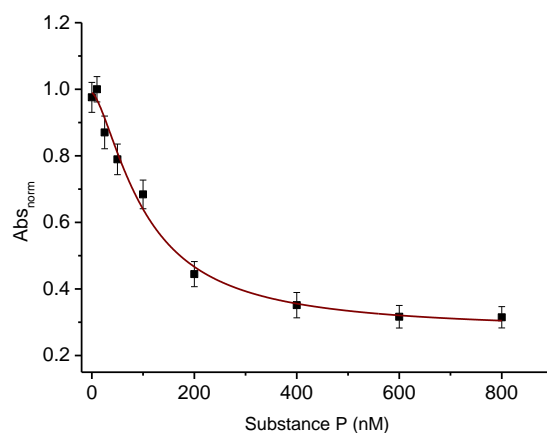


Figure Error! No text of specified style in document.-11 Affinity profiles in bio-GHR experiments (223 nM) and different concentrations of Substance P. All experiments were performed in triplicate in 10 mM PBS buffer, pH 7.4, at 37 °C.

LOD for Substance P was found 23.0 ng/mL.

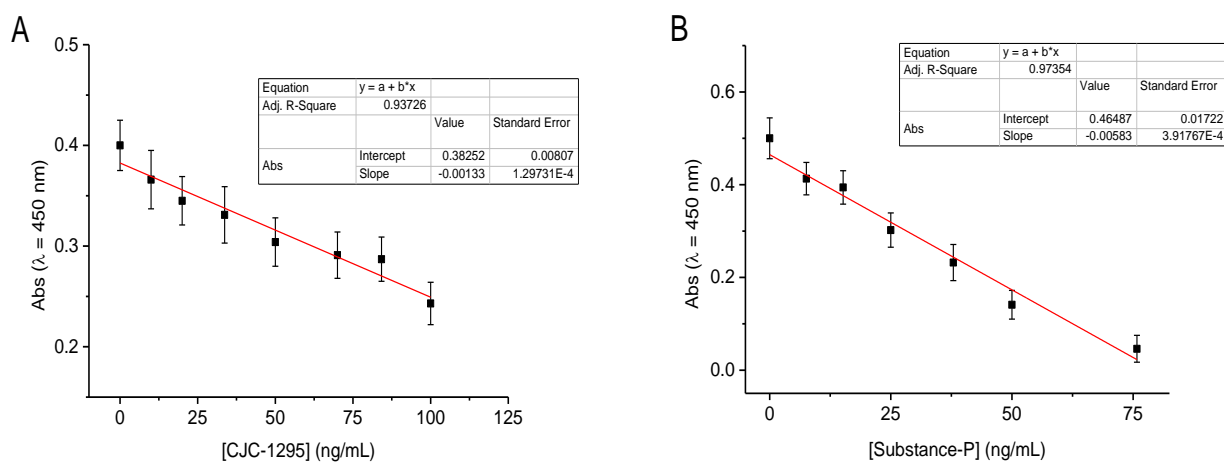


Figure Error! No text of specified style in document.-12 Calibration plots obtained in 10 mM PBS buffer, pH 7.4, at 37 °C for (A) CJC-1295-DAC agonist and (B) Substance P inverse agonist. The correlation coefficients obtained were (A) $R^2 = 0.93726$ and (B) $R^2 = 0.97354$

Chapter 4 - Detection of allosteric modulators such as natural cannabinoids

Cannabinoids are organic compounds with chemical structures of 21 carbon atoms and a terpenophenolic backbone (Abd-Elsalam et al., 2019, Klimuntowski et al., 2020). Δ^9 -tetrahydrocannabinol (**THC**) and cannabidiol (**CBD**) are the most common and well-known cannabinoids (Alves et al., 2020).

To the best of our knowledge, no affinity systems have been reported in the literature between the GHSR-1a receptor and cannabinoids as allosteric modulators.

The modulating effect of cannabinoids

The existence of a modulating effect of carboxy-THC and CBD at GHS-R1a receptor was investigated using the affinity profiles. Cannabinoids may interact with GHSR-1a allosteric sites, either by promoting the binding of ghrelin to the orthosteric site or by blocking its binding.

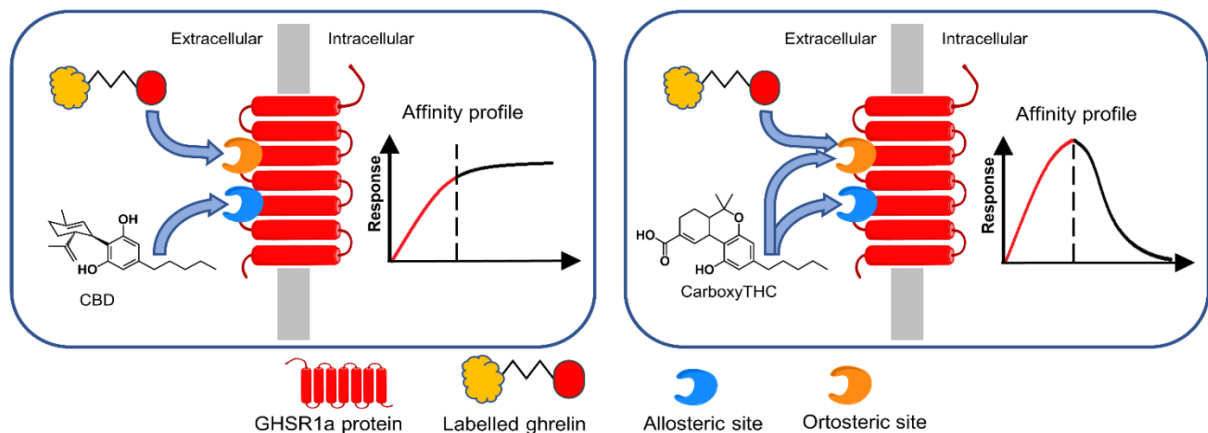


Figure Error! No text of specified style in document.-13 Schematic representation of sensing format for carboxy-THC and CBD

Affinity profiles of allosteric modulators

The binding curves of cannabinoids in direct competitive experiments with labeled ghrelin were analyzed by nonlinear regression analysis using the Hill equation (Sebaugh, 2011) (Figure 4-2).

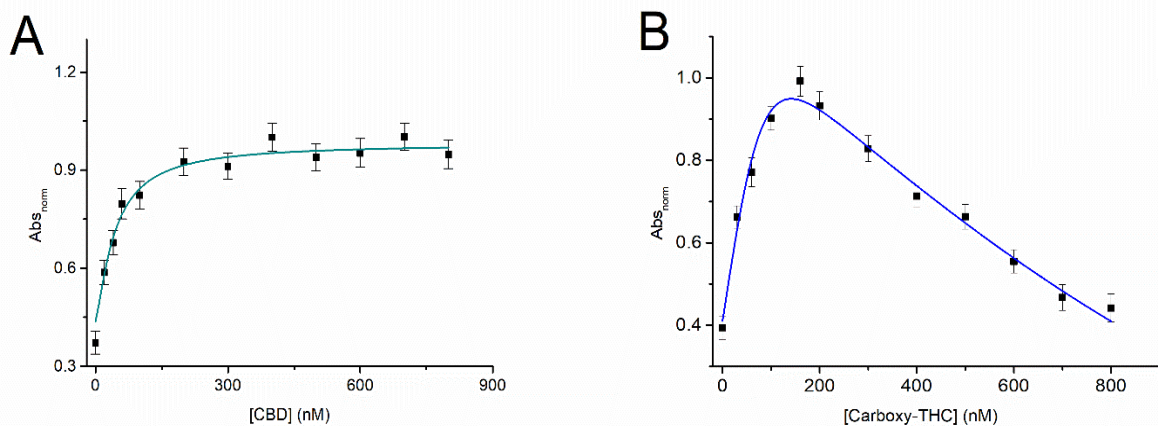


Figure Error! No text of specified style in document.-14 Affinity profiles in experiments with 223 nM bio-GHR and different concentrations of (A) CBD and (B) Carboxy-THC. All experiments were performed in triplicate in 10 mM PBS buffer, pH 7.4 at 37 °C.

It can be noticed that the affinity profiles of CBD and carboxy-THC show distinct features: the CBD hyperbolic - and the carboxy-THC bell-shaped patterns suggest that cannabinoids are much likely to interact with two distinct regions of GHS-R1a in competitive experiments.

To date, there are no data providing direct evidence of an allosteric site for extracellular ligands binding in GHS-R1a, although such behavior has been reported for other transmembrane receptors (Conn et al., 2009).

The values estimated for the dissociation constants for the two allosteric modulators are shown in Table 4-1.

Table Error! No text of specified style in document.-4 Dissociation constants obtained for CBD and carboxy-THC in the corresponding systems of linear equations

Dissociation constant (nM)	CBD	Carboxy-THC
K_1^{-1} (determined in direct experiments with GHR)	88.90 ± 0.63	88.90 ± 0.63
K_2^{-1} (determined in competitive experiments with modulators)	-	(3.94 ± 0.35) × 10 ⁸
K_3^{-1} (determined in competitive experiments with modulators)	3082 ± 76	234 ± 13
K_4^{-1} (determined in competitive experiments with modulators)	1.150 ± 0.009	135 ± 9
K_5^{-1} (determined in competitive experiments with modulators)	-	0.705 ± 0.071
K_6^{-1} (determined in competitive experiments with modulators)	-	60.1 ± 3.2

CBD and carboxy-THC display low affinity for the allosteric site (K_3^{-1}), the formation of the RM* activated complex being favored in the case of the carboxy-THC. The estimated values for K_4^{-1} of 135 nM for carboxy-THC and 1.15 nM for CBD, confirm that the binding of ghrelin to the CBD-receptor complex is more favorable compared to carboxy-THC-receptor complex.

Calibration lines were plotted within 5 - 30 ng/mL range, where possible interferences of GHR mimetics are minimized (Figure 4-4).

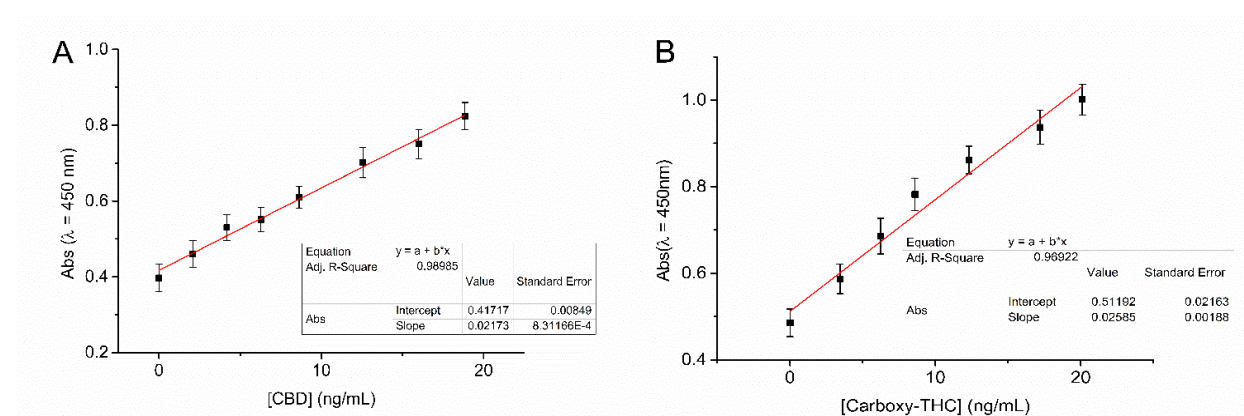


Figure Error! No text of specified style in document.-15 Calibration lines for (A) CBD and (B) carboxy-THC PBS 10 mM, pH 7.4 and 37 °C

A LOD for CBD of 5.1 ng/mL and 3.7 ng/mL for carboxy-THC were obtained. Spiked samples with the two cannabinoids in a 1: 4 (v/v) mixture of synthetic urine:PBS were analyzed (Figure 4-5).

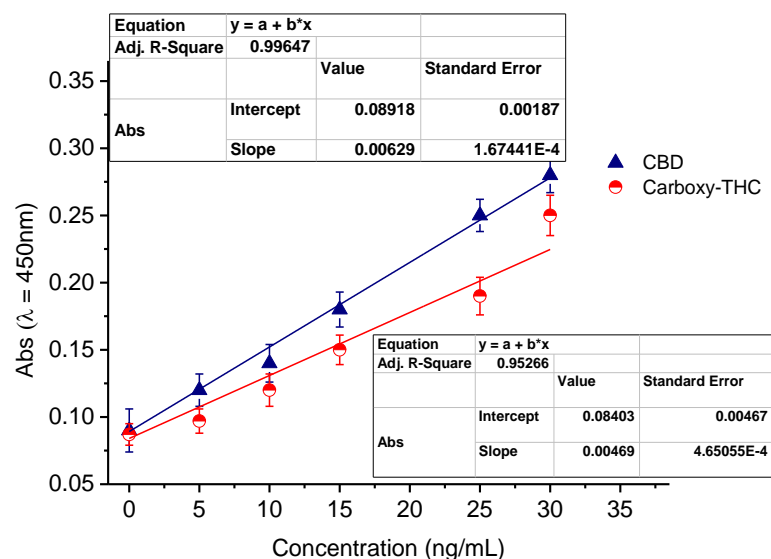


Figure Error! No text of specified style in document.-16 Calibration lines for CBD and carboxy-THC in 1:4 (v/v) mixture of synthetic urine:10 mM PBS buffer, pH 7.4 and 37 °C. The experiments were performed in triplicate.

Similar values were obtained in the synthetic urine mixture for the detection limits: 7.63 ng/mL for CBD and 5.12 ng/mL for carboxy-THC.

Validation of the affinity profile-based method by comparison with the gas-chromatographic coupled with tandem mass spectrometry method

The validation of results obtained by the direct competitive method, based on affinity profiles, was performed by gas-chromatographic technique coupled with tandem mass spectrometry (GC-MS/MS) based on the physical and chemical properties of the analytes (Table 4-2).

Table Error! No text of specified style in document.-5 Physical and chemical properties of CBD and carboxy-THC

Analyte	Chemical formula	Molecular Weight (Da)	Groups available for silylation	Molecular mass + 2-TMS
CBD	C ₂₁ H ₃₀ O ₂	314	2-OH	458
Carboxy-THC	C ₂₁ H ₂₈ O ₄	344	2-OH	488

Figure 4-6 shows a total chromatogram ion (TIC) of the studied analytes and the two internal standards (D4-Androsterone and D5-Etiocholanolone) to monitor the enzymatic hydrolysis step and the derivatization process. D9-THC was used as internal standard for the quantitation.

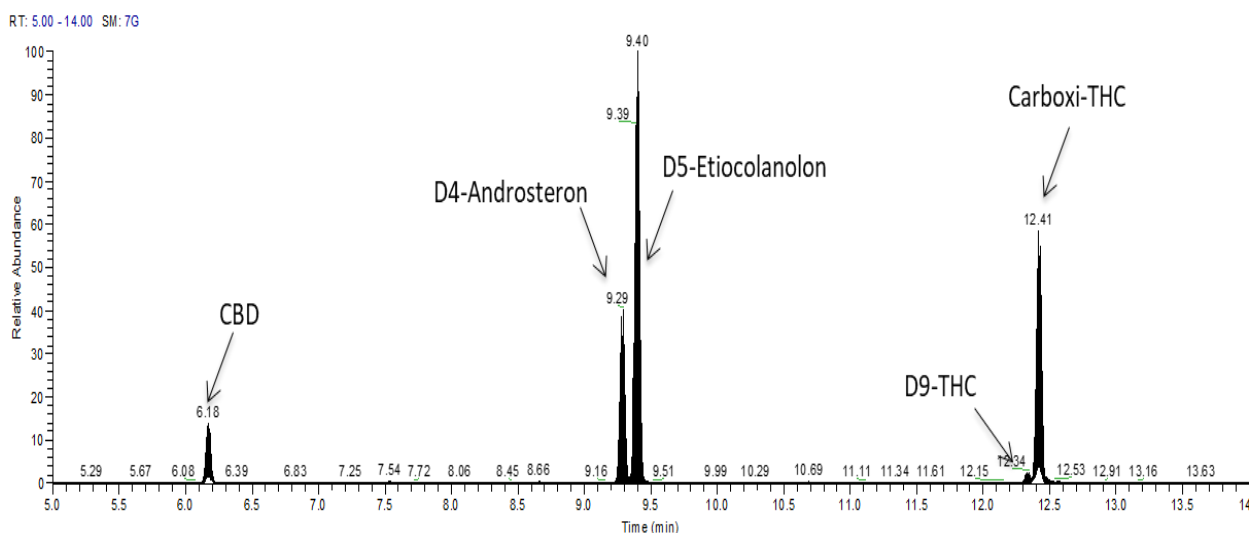


Figure Error! No text of specified style in document.-17 Total Ion Chromatogram (TIC) obtained for simultaneous detection of CBD (retention time 6.18 minutes) and carboxy-THC (retention time 12.41 minutes). D4-Androsteron and D5-Etiocolanolon were internal standards to monitor the enzymatic hydrolysis step and the derivatization process.

The results of the optimization steps are presented in Table 4-4.

Table Error! No text of specified style in document.-6 Optimized transitions and collision energies for the quantification of CBD and Carboxy-THC.

Cannabinoid	Relative retention time	Mass transition	Collision energy (eV)
Carboxy-THC	1.01	473.3 - 355.2	19
CBD	0.50	390.3 - 319.2	12
D9-THC (internal standard)	1.00	380.2 - 292.1	17

The quantitation of the two natural cannabinoids was performed using a 8-point calibration line for CBD and carboxy-THC within 0 and 100 ng/mL, both in 10 mM PBS buffer, pH 7.4, and in 1:4 synthetic urine:PBS mixture (Figure 4-9). The calibration was used to compare the results obtained with the chromatographic method and with the method based on the affinity profiles.

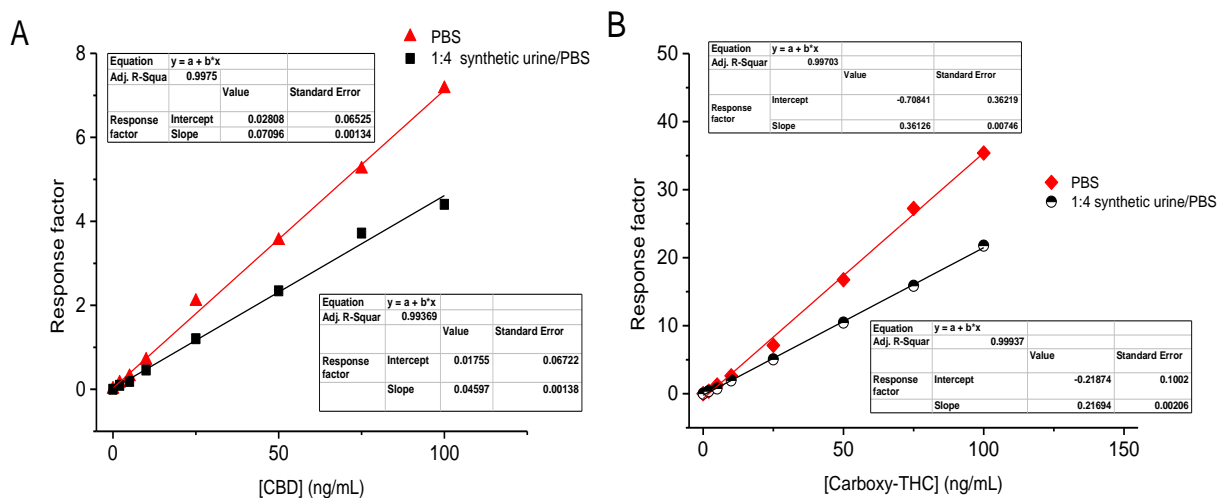


Figure Error! No text of specified style in document.-18 Matrix influence on the sensitivity of GC-MS/MS detection as resulted from the calibration lines of A) CBD and B) Carboxy-THC in PBS and in 1:4 diluted urine samples with PBS. The response factor was defined as the ratio between the peak area of the analyte and the peak area of the internal standard

Similar results were obtained by both analytical methods (Table 4-6), confirming that the affinity-based detection format provides highly reliable results.

Table *Error! No text of specified style in document.-7* Comparative results on CBD and carboxy-THC detection by spectrophotometric method and GC-MS/MS in spiked samples prepared in PBS buffer and 1:4 synthetic urine / PBS buffer mixture

Analyte	Competitive affinity format		GC-MS/MS	
	sample in PBS±SD (ng/mL)	sample in 1:4 synthetic urine / PBS mixed ± SD (ng/mL)	sample in PBS±SD (ng/mL)	sample in 1:4 synthetic urine / PBS mixed ± SD (ng/mL)
CBD	14.89± 0.11	15.22± 0.13	15.060± 0.054	14.980± 0.047
Carboxy-THC	15.13± 0.14	15.18± 0.14	15.050± 0.061	15.020± 0.031

Chapter 5 - Implementation of the receptor / agonist affinity pair on molecular wire as conductive support for the electrochemical detection of doping control substances

This chapter presents the development of a modular peptide sensor using a gold electrode on which a stable, conductive system, characterized by an efficient and fast electron transfer was implemented. A 9-mer peptide containing alternating polar and ionisable side chains and constrained to a α -helix configuration was used.

Biosensor development principle

The modular format of the biosensor (Figure 5-1) required successive electrochemical, chemical and affinity steps.

Surface activation

The gold electrodes used in electrochemical experiments were electrochemically cleaned using successive steps of cyclic voltammetry and chronoamperometry.

Determination of electrochemically active surface area (ESA)

The oxygen adsorption measurement was chosen to obtain an indication of the microscopic surface area for gold. ESA was calculated as the ratio between the charge of the gold oxide reduction presented on the studied electrode surface ($Q_{Au/\alpha}$ oxide) and Q_{Std} .

Monitoring the formation of the mixed SP/MCH film and the chemisorption of the MB redox reporter

The formation of SP/MCH was monitored by CV using 1 mM $K_3Fe(CN)_6$ in 1 M KCl with potential scans from 0 to 0.6 V with a scan rate of 0.1 Vs^{-1} . The chemisorption of the MB-NHS ester to the SP/MCH film was investigated using square wave voltammetry (SWV).

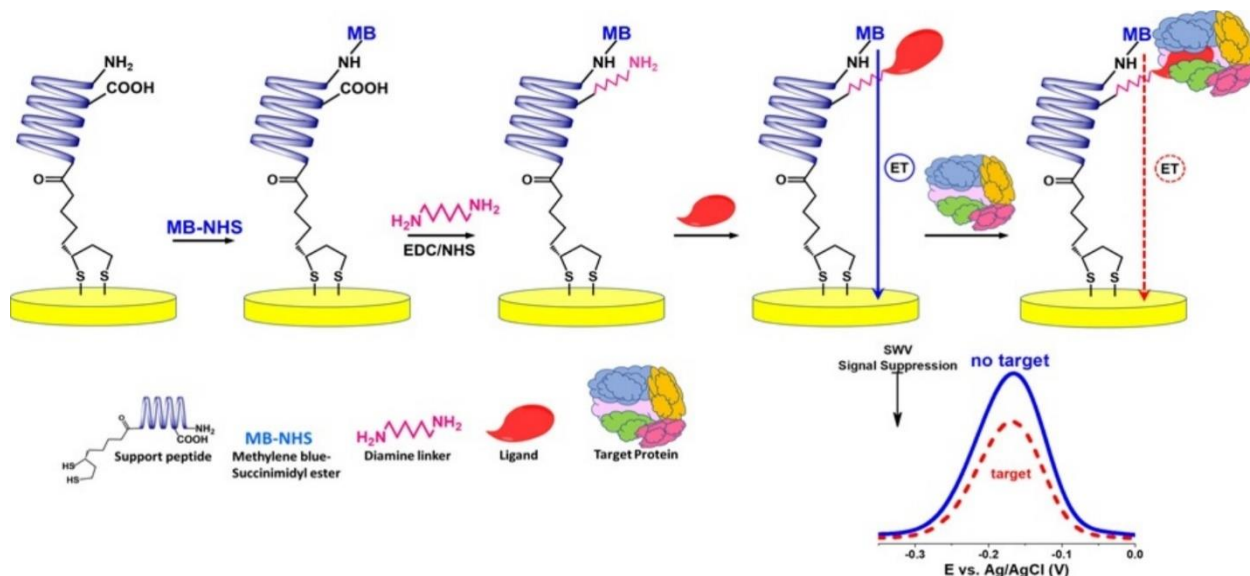


Figure Error! No text of specified style in document.-19 Biosensor development and detection principle: deposition of the peptide layer onto rough surface, labelling on-the-fly with MB, covalent attachment of diamino-linker at a glutamate residue below the MB label and immobilization of ligand; the specific interaction ligand/high-molecular weight target hampers the electron transfer from MB to the electrode's surface, thus suppressing the MB signal in SWV.

Estimation of surface coverage of chemisorbed MB

To estimate the area occupied by MB, measurements were performed using:

- CV within -0.55 and 0 V vs. Ag/AgCl in 100 mM PBS, with the scan rate varying from 10 to 1000 mV/s;
- ACV within 0 and -0.55 V vs. Ag/AgCl in 100 mM PBS.

The characterization of the surface modification was achieved using both cyclic voltammetry and electrochemical impedance spectroscopy.

Labelling the SP-modified electrode with MB

The electrode modified with the support peptide layer was incubated with 100 μL of 200 μM MB-NHS solution in 10 mM bicarbonate buffer pH 8.5 (containing 22 % v/v DMF) for 30 minutes.

Immobilization of agonist onto MB/SP/MCH modified electrode

The immobilization of CJC-1295-DAC was achieved through the free carboxyl group on the peptide layer that was pre-activated *via* EDC/NHS esters (pH = 9) to bind the unprotonated

groups of EDA or HMDA linkers. Then, the free amino groups were functionalized with the maleimide-CJC at pH = 8.5.

Long-term storage of sensors and regeneration of the sensor surface

When not in use, the sensors were stored in 0.1 M PBS solution containing 2.5% glycerol at 4 °C.

The optimal surface regeneration solution was 0.1 M NaCl solution with the addition of 0.1% Tween 20 for 15 minutes. A recovery within 96–98 % of the initial signal was observed.

Design of the peptide bridge

The peptide support consisted of a rich alanine-based peptide sequence (X-YAAAHAEAK-NH₂ where X is a lipoyl residue) constrained to α -helical structure, with the overall dipole moment oriented from the electrode surface to the other end of the peptide.

Thus, the results of the circular dichroism spectrum of a solution of support peptide processed with the CONTIN analysis algorithm in Dichroweb (Whitmore and Wallace, 2008, Sreerama and Woody, 2000), shows that the peptide has a 98.8% α -helix content.

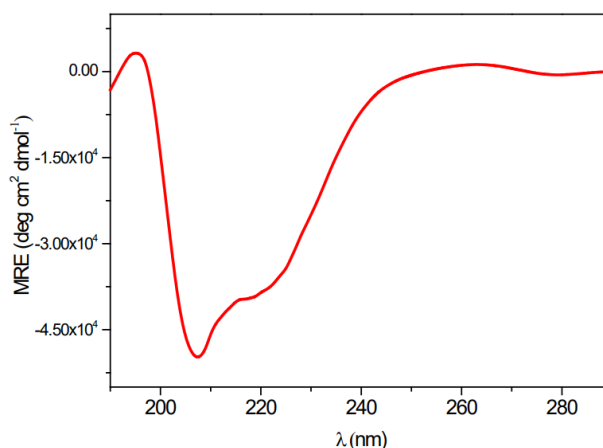


Figure Error! No text of specified style in document.-20 Circular dichroism spectrum of 100 μ M SP in acetonitrile. The negative peaks at 207 and 222 nm sustain the hypothesis of an α -helix configuration.

Optimization of the pre-treatment procedure

The electrochemical steps were optimized to provide a reproducible ESA and to ensure the formation of a stable peptide support. A reproducible value of the roughness factor (Rf, defined as the ratio between ESA and the geometric area of the electrode's surface). This value was 1.6 ± 0.11 ($n = 4$ electrodes). The results obtained are shown in Figure 5-3.

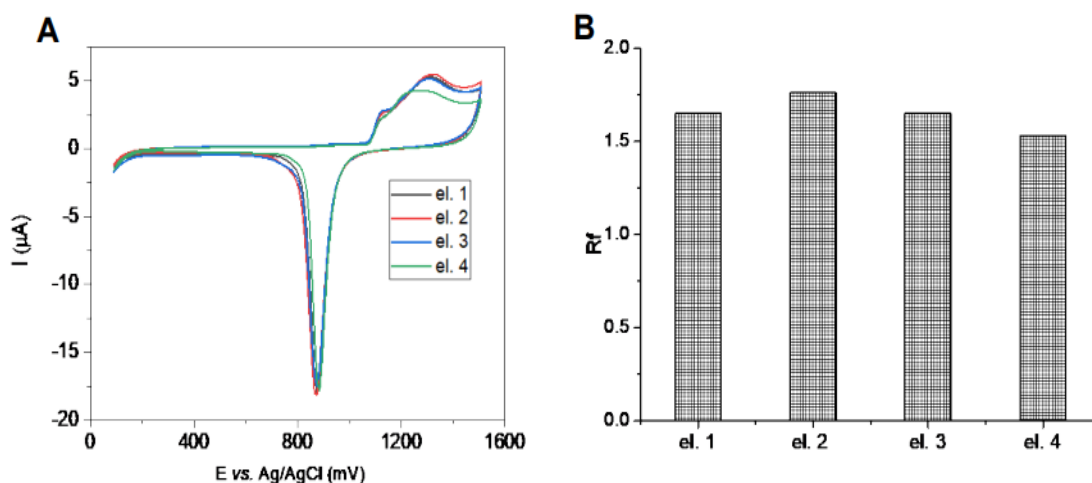


Figure Error! No text of specified style in document.-21 (A) Determination of ESA for 4 gold rod electrodes through CV measurements in 0.05 M H_2SO_4 ($v = 0.1 \text{ V s}^{-1}$); (B) Roughness factors obtained after surface activation using the combined procedures: CV scans in basic and acidic conditions followed by a triple-potential pulse waveform in 100 mM PBS

Construction and characterization of the peptide bridge

The formation of the peptide film on the electrode surface, prior to MB labeling, was monitored through CV measurements in $\text{K}_3\text{Fe}(\text{CN})_6$ solution. The formation of an insulating peptide layer was investigated at different SP densities within 50 - 100 μM and 1 mM MCH (Figure 5-4).

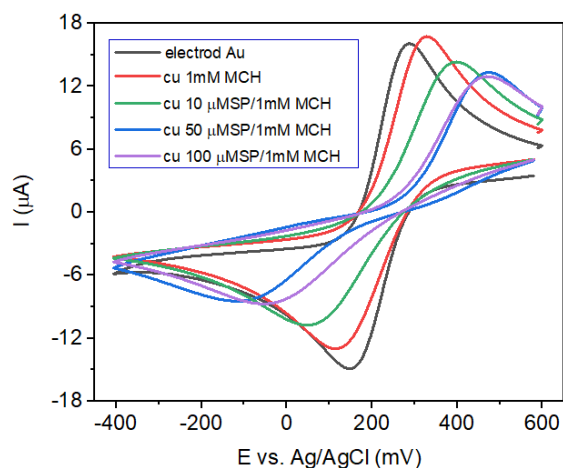


Figure Error! No text of specified style in document.-22 CV responses of the SP/MCH-modified electrodes in 1mM $\text{K}_3\text{Fe}(\text{CN})_6$ / 1M KCl, following an 18-hour incubation of electrodes in SP/MCH solutions (scan rate 100 mV/s)

The number of moles of surface confined MB (N) was determined from the CV and ACV measurements and the results obtained by both voltammetric techniques are similar, as can be seen from Table 5-1.

Table Error! No text of specified style in document.-8 Surface coverages of mixed MB/SP/MCH determined through the surface-confined MB signaling in CV and ACV (triplicate experiments)

SP (μM)	Surface coverage of bound MB $\Gamma \times 10^{11}$ (mol/cm^2)	
	CV	ACV
100	2.52 ± 0.11	3.78 ± 0.16
50	3.61 ± 0.31	4.91 ± 0.22
10	0.911 ± 0.047	1.060 ± 0.034
0	0.488 ± 0.035	0.504 ± 0.035

Estimation of the kinetic parameters of the electron transfer

In Figure 5-6, the characteristic voltammograms of the MB / SP / MCH system are represented, with well-developed voltammetric peaks for the anodic current (I_f), for the cathodic current (I_b) and for the differential net current (I_{net}). Voltammetric features correspond to the typical behavior of a quasi-reversible electrode reaction of an immobilized redox couple.

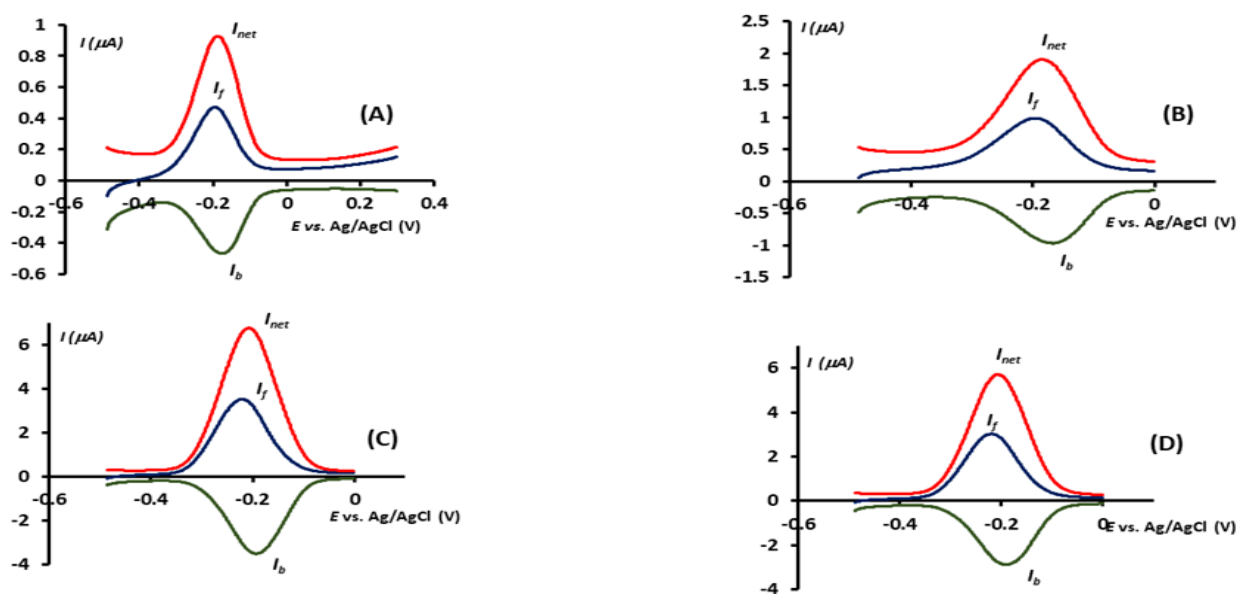


Figure Error! No text of specified style in document.-23 Typical SW voltammetric response of MB immobilized on the electrode surface in the absence (A) and in the presence of SP at concentration of 10 μM (B), 50 μM (C) and 100 μM (D): net (I_{net}), forward (I_f) and backward (I_b) currents). The parameters of the potential modulation were $f=25$ Hz, $E_{sw}=50$ mV and $\Delta E_{step}=1.5$ mV. The SWVs were recorded in 100 mM PBS, in overall anodic directions starting from -0.500 V.

The most important parameters of the voltammograms shown in Figure 5-6 are presented in Table 5-2.

Table Error! No text of specified style in document.-9 Parameters characteristic of SVW voltammograms shown in Figure 5-6

System	$I_{net, p}$ (μA)	E_p (V)	ΔE_p (mV)	$I_{p,b}/I_{p,f}$	α_1
--------	--------------------------------	-----------	-------------------	-------------------	------------

MB / MCH	0.789	-0.190	18	0.836	0.630
MB / 10 μ M SP / MCH	1.51	-0.180	26	0.956	0.540
MB / 50 μ M SP / MCH	6.56	-0.204	29	0.978	0.520
MB / 100 μ M SP / MCH	5.39	-0.205	29	0.935	0.550

The position of the maximum in the presence of peptide is at higher frequencies, clearly revealing an increased standard rate constant, compared to the case of the system in the absence of SP (Figure 5-8).

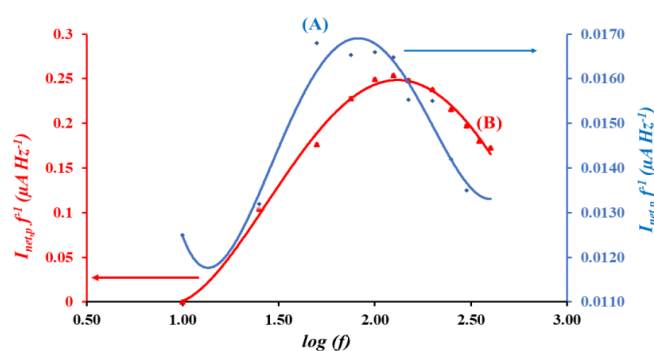


Figure Error! No text of specified style in document. -24 Quasi-reversible maximum of MB in absence (curve (A), right ordinate) and in the presence of 50 μ M of the support peptide (curve (B), left ordinate). The other parameters are SW amplitude $E_{sw} = 25$ mV and step potential $\Delta E_{step} = 1.5$ mV.

Stability of the peptide layer

The stability of the MB/SP/MCH system was monitored over within 25 days after MB functionalization. After a drop of 22 % in the first day, the signal decreased slowly to a percent of 73 % (from the initial value).

Detection of growth hormone secretatgog receptor

The CJC-1295 on MB/SP/MCH was immobilized through covalent bonding to the diamino-linker attached to a free carboxyl group from the glutamate residue. When using EDA as linker a 22 % signal suppression (SS) at 50 ng/mL GHS-R1a binding was observed, while the use of HMDA yielded 33.5 % SS for the same concentration of GHS-R1a (Figure 5-15).

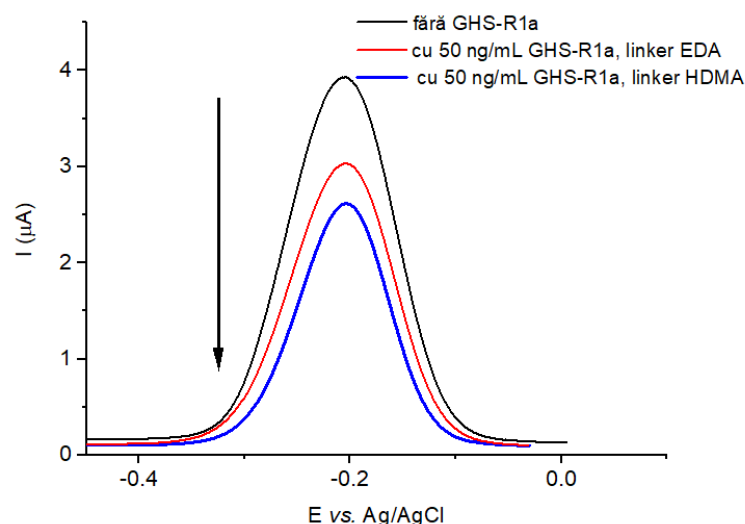
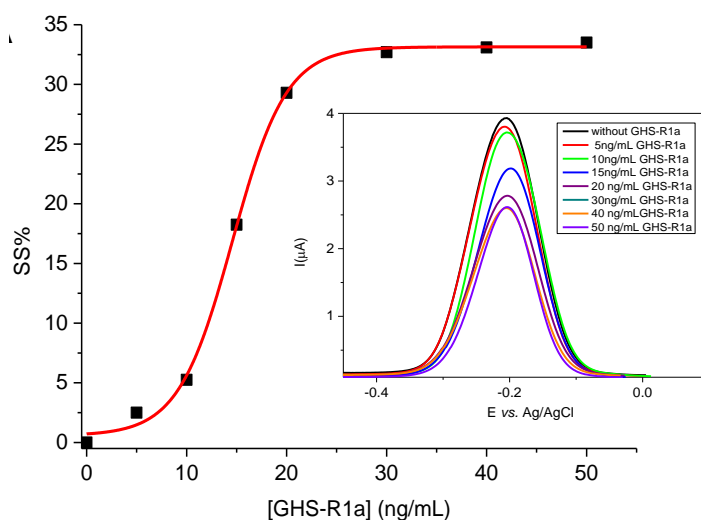


Figure Error! No text of specified style in document.-25 Decrease of SWV current at the binding of the GHSR-1a to the CJC-1295 immobilized onto MB/SP/MCH electrode using two different linkers: ethylenediamine and hexamethylenediamine (SWVs recorded in 100 mM PBS, $E_{sw} = 25$ mV, $\Delta E_{step} = 1.5$ mV, and $f = 25$ Hz). The experiments were performed in 100 mM PBS, pH= 7.4, T = 298 K.

The binding of the ghrelin receptor to the immobilized ligand leads to a signal decrease which is concentration-dependent, this effect being illustrated by experiments with increasing receptor concentrations in the range of 5 - 50 ng/mL (Figure 5-16).



FigureError! No text of specified style in document.-26 Sigmoidal shaped patterns of signal suppression vs. target concentration, following the target binding to the immobilized ligand onto MB/SP/MCH support for GHS-R1a and (inset SWVs recorded in 100 mM PBS, pH = 7.4). The experiments were performed in PBS, pH = 7.4, T = 298 K.

The best-fit parameters were:

$b = 249 \pm 23$ pM (corresponding to 14.4 ± 1.3 ng/mL);

$c = 2.5 \pm 0.3$ (with $R^2 = 0.978$)

Reproducibility, anti-interference, and selectivity studies

Reproducibility studies were performed on the functionalized sensor, in the presence of the GHSR-1a receptor at a concentration of 15 ng/mL, from the signal suppression on SWV and using 3 gold electrodes. The biosensor showed good reproducibility with a relative standard deviation (RSD) of 2.5%.

The anti-interference performance of the biosensor was evaluated in the presence of two non-specific antibodies: anti-Ochratoxin A and anti-Chloramphenicol, and the signal suppression for each antibody was compared to the signal suppression due to the specific binding of the target. It was noticed that SS is significant in the presence of the target (around 33%), exceeding the signal changes caused by non-specific binding (only 3% for anti-Ochratoxin A and 9% for anti-chloramphenicol).

A selectivity test was performed further on mixtures containing the target analyte and the non-specific antibodies. The SWV signal recorded in these mixtures were almost the same as in the solutions containing just the analyte, confirming the selectivity of the fabricated biosensors (Figure 5-18).

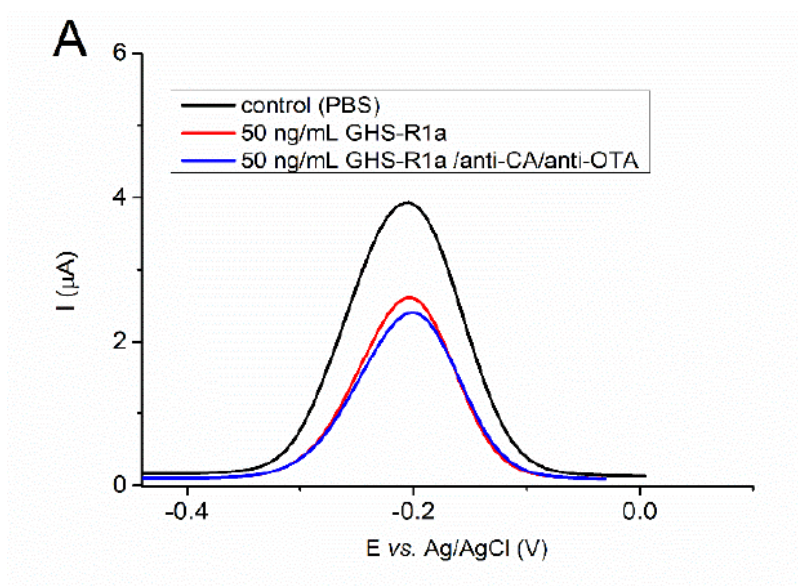


Figure Error! No text of specified style in document.-27 Selectivity test for GHS-R1a detection in the presence of non-specific antibodies, anti-Ochratoxin A and anti-Chloramphenicol.

GENERAL CONCLUSIONS AND PERSPECTIVES

The doctoral thesis aimed the development of affinity formats for the rapid detection, *screening* type detection methods for several compounds whose administration may enhance performance in sport. For this purpose, detection formats have been developed for ghrelin mimetics such as the peptide agonist CJC-1295-DAC, inverse to the agonist [D-Arg¹, D-Phe⁵, D-Trp^{7,9}, Leu¹¹]-Substance P, the peptide antagonist [D-Lys³]-GHRP-6 and the two antagonists with non-peptide structure: YIL-781 and L-692,585, exploiting the specific interaction with the secretagogue growth hormone receptor, GHS-R1a. The analysis protocol allowed a better understanding of the mechanism of interaction of the secretagogue receptor with the extracellular ligands.

Ligand-receptor affinity constants were estimated, and the analytes could be detected in diluted urine samples, which did not require prior extraction steps. The detection limits obtained were [D-Lys³]-GHRP-6 - 29.0 ng/mL, and for YIL-781 - 27.0 ng/mL.

GHSR-1a antagonists, at low concentrations, activate the receptor. This promoting effect of the receptor activity has a major impact on human metabolism and can be applied in weight control and reduction of body fat mass, but also in the treatment of eating disorders.

We studied affinity profiles of the peptide agonist CJC-1295-DAC and inverse agonist [D-Arg¹,D-Phe⁵,D-Trp^{7,9}, Leu¹¹]-Substance P. Affinity constants were estimated using nonlinear regression analysis. The detection limits were: for [D-Arg¹,D-Phe⁵,D-Trp^{7,9}, Leu¹¹]-Substance P- 23.0 ng/mL, for CJC-1295-DAC - 56.0 ng/mL.

The analysis format based on the analysis of affinity profiles also gave good results in the case of two cannabinoids, CBD, and carboxy-THC. They function as allosteric modulators of the GHSR-1a receptor, which is a novelty in the field. This method can detect CBD and the major metabolite of THC in dilute urine samples. The detection limits were 5.1 ng/mL for CBD and 3.7 ng/mL for carboxy-THC; the experimental results were validated using the GC-MS/MS technique (the standard method used by doping control laboratories).

In the last chapter we studied the conductive properties of a peptide sequence consisting of 9 amino acids in order to develop an electrochemical affinity bisensor for the detection of ghrelin receptor. The peptide was deposited on a gold electrode, forming a thin film on the surface. The controlled immobilization of the redox marker, Methylene Blue, on the peptide support was monitored by voltammetric techniques (CV, ACV and SWV) which subsequently confirmed the existence and stability of the peptidic layer on the surface of the gold electrode.

The peptide agonist, CJC-1295-DAC and the GHSR-1a receptor, were used successfully to illustrate the possibility of electrochemical detection of these analytes according to their specific interaction. The sensor does not require the labeling of ligands or target molecules, and the detection is based on the signal suppression recorded for the redox marker, MB immobilized on the peptide support. The estimated limit of detection was 14.4 ng/mL.

List of published articles in the PhD thesis research topic

Articles published in ISI listed journals

1. Early detection of growth hormone secretagogue receptor antagonists exploiting their atypical behavior in competitive assays, **George Mădălin Dănilă**, Mihaela Puiu, Lucian-Gabriel Zamfir, Camelia Bala, *Analytical Chemistry*, 2019, 91 (23), 14812-14817 (Impact Factor: 6.785)
2. Early detection of cannabinoids in biological samples based on their affinity interaction with the growth hormone secretagogue receptor, **George Mădălin Dănilă**, Mihaela Puiu, Lucian-Gabriel Zamfir, Camelia Bala, *Talanta*, 2021, 237:122905 (Impact factor: 6.057)
3. Label-free detection of target proteins using peptide molecular wires as conductive supports, Mihaela Puiu, Lucian-Gabriel Zamfir, **George Mădălin Dănilă**, Francesco Papi, Cristina Nativi, Valentin Mirceski, Camelia Bala, *Sensors and Actuators B: Chemical*, 2021, 345, 130416 (Impact factor: 7.460)

SELECTED REFERENCES

- ABD-ELSALAM, W. H., ALSHERBINY, M. A., KUNG, J. Y., PATE, D. W. & LÖBENBERG, R. 2019. LC-MS/MS quantitation of phytocannabinoids and their metabolites in biological matrices. *Talanta*, 204, 846-867.
- ALVES, P., AMARAL, C., TEIXEIRA, N. & CORREIA-DA-SILVA, G. 2020. Cannabis sativa: Much more beyond $\Delta(9)$ -tetrahydrocannabinol. *Pharmacological Research*, 157, 104822.

- CONN, P. J., CHRISTOPOULOS, A. & LINDSLEY, C. W. 2009. Allosteric modulators of GPCRs: a novel approach for the treatment of CNS disorders. *Nature Reviews Drug Discovery*, 8, 41-54.
- HOLST, B., CYGANKIEWICZ, A., JENSEN, T. H., ANKERSEN, M. & SCHWARTZ, T. W. 2003. High constitutive signaling of the ghrelin receptor--identification of a potent inverse agonist. *Molecular Endocrinology*, 17, 2201-10.
- KLIMUNTOWSKI, M., ALAM, M. M., SINGH, G. & HOWLADER, M. M. R. 2020. Electrochemical sensing of cannabinoids in biofluids: A noninvasive tool for drug detection. *ACS Sensors*, 5, 620-636.
- PUIU, M., ZAMFIR, L.-G., BUICULESCU, V., BARACU, A., MITREA, C. & BALA, C. 2018. Significance testing and multivariate analysis of datasets from surface plasmon resonance and surface acoustic wave biosensors: prediction and assay validation for surface binding of large analytes. *Sensors*, 18.
- SARTORE, D. M., VARGAS MEDINA, D. A., COSTA, J. L., LANÇAS, F. M. & SANTOS-NETO, Á. J. 2020. Automated microextraction by packed sorbent of cannabinoids from human urine using a lab-made device packed with molecularly imprinted polymer. *Talanta*, 219, 121185.
- SEBAUGH, J. L. 2011. Guidelines for accurate EC50/IC50 estimation. *Pharmaceutical Statistics*, 10, 128-134.
- SREERAMA, N. & WOODY, R. W. 2000. Estimation of protein secondary structure from circular dichroism spectra: comparison of CONTIN, SELCON, and CDSSTR methods with an expanded reference Set. *Analytical Biochemistry*, 287, 252-260.
- WHITMORE, L. & WALLACE, B. A. 2008. Protein secondary structure analyses from circular dichroism spectroscopy: Methods and reference databases. *Biopolymers*, 89, 392-400.